U.S. Department of the Interior
US. Geological Survey

Age and paleomagnetism of basaltic lava flows in corehole ANL-OBS-AQ-014 at Argonne National Laboratory-West, Idaho National Engineering and Environmental Laboratory

by

Duane E. Champion and Marvin A. Lanphere
U. S. Geological Survey
345 Middlefield Road, Menlo Park, CA 94025

Open-File Report 97-700

ABSTRACT

The age and paleomagnetism were determined on basalt from 27 lava flows represented in about 1,900 feet of core from corehole ANL-OBS-AQ-014 in the area of the Argonne National Laboratory-West facilities of the Idaho National Engineering and Environmental Laboratory (INEEL). Paleomagnetic study was also made on an additional core from a shallow corehole located a mile east of that facility. Paleomagnetic measurements were made on 462 samples from the two coreholes, which are compared to each other, and to surface outcrop paleomagnetic data. $^{40}Ar/^{39}Ar$ measurements were made on 5 basalt samples over the length of core ANL-OBS-AQ-014, and these samples range in age from 565 ka to 1.75 Ma. The pattern of accumulation suggested by these ages is irregular. Very rapid rates (>3,000'/m.y.) quickly piled up hundreds of feet of lava in different time-separated events, interspersed with eruptive hiatuses, some of which may have lasted 650 k.y.

INTRODUCTION

The U.S. Geological Survey currently is studying the petrography, paleomagnetism, and age of basalt lava flows in numerous coreholes at the Idaho National Engineering and Environmental Laboratory (INEEL). The INEEL is located between Arco and Idaho Falls in southeastern Idaho (Fig. 1). The current program is a continuation of studies begun in 1974 to evaluate potential volcanic hazards at INEEL. These studies have included geologic mapping and various studies of surface lava flows such as petrologic and paleomagnetic investigations and radiometric age measurements. Previous investigations also were carried out on selected drill cores from different facilities located within the INEEL.

The present project was begun in Spring, 1996 with the objective of studying, in some detail, core samples from a new deep well, ANL-OBS-AQ-014, located just west of the Argonne National Laboratory-West facilities in the INEEL. This core will hereafter be referred to as {014}. This work was done in collaboration with the Idaho Universities Consortium of the Idaho Water Resources Research Institute (IWRRI), with the purpose of understanding the basalt stratigraphy of the SE corner of INEEL, for which no coring of any significance had been done

previously. This information will be used to extend a three-dimensional stratigraphic framework of the INEEL for geologic and hydrologic studies, including the evaluation of potential volcanic hazards to the Argonne facilities and the movement of radionuclides in the Snake River aquifer. Funding for this research has been provided by the U.S. Department of Energy, through IWRRI.

GEOLOGIC SETTING

The INEEL covers an area of about 2,300 km^2 in the eastern Snake River Plain (Fig. 1), which is a northeast-trending structural trough containing Neogene volcanic rocks and interbedded sediments. Tertiary rhyolites are generally exposed only along the margins of the Plain, but several Quaternary rhyolite domes, surrounded by basalt flows, are located in the Plain. Most of the eastern Snake River Plain is covered by late Pleistocene and Holocene basalt lava fields. In particular, the axis of the Plain is a continuing locus of the basalt shield vents from which these young lavas erupt. Kuntz and others (1994) showed that the surface area of the Argonne-West facility is dominated by lava flows of their Qbc relative age classification unit, suggesting they are 200 to 400 ka in age.

ANALYTICAL TECHNIQUES

The drill core from well {014} was carefully logged and sampled. The logging involved a basic description of core material and location of tops and bottoms of lava flows. Depths were measured by tape measure from known depths recorded on wooden plugs in the core boxes. This study doesn't include the detailed depth, thickness and petrographic descriptions that were part of our previous studies; these descriptions will be presented at a later time by Kuntz.

For paleomagnetic studies, seven samples of core, generally 6 cm in diameter were taken from each flow. For each sample, a 2.5 cm diameter core was drilled at right angles to the axis of the original core to provide material for paleomagnetic analysis. A gyroscopic deviation log of the well was made at 10' intervals, and it reveals that the hole deviates no more than 1.4° from the vertical over it's length and more usually less than a degree. Thus these mini-core samples can be assumed horizontal in orientation with reasonable accuracy. The samples were trimmed

to 2.2 cm lengths, and the inclination and intensity of magnetization were measured with a cryogenic magnetometer.

Thin sections of 15 samples of basalt from core {014} were examined petrographically to determine those most suitable for $^{40}Ar/^{39}Ar$ dating. Five samples were chosen for analysis; these samples met the usual criteria of acceptability for argon dating (Dalrymple and Lanphere, 1969; Mankinen and Dalrymple, 1972). The samples were selected to minimize the amount of glass in the groundmass. Of those samples selected, glass in the groundmass was considered too small in volume to affect the measurements. The samples were crushed and ground to a size of 1/2 to 1 mm. Splits of the whole-rock samples were packaged in copper foil, and placed in cylindrical vials along with mineral grains of known age. In the $^{40}Ar/^{39}Ar$ method, the sample is irradiated with fast neutrons, along with a monitor mineral of known age, to induce the reaction $^{39}K(n,p)^{39}Ar$. The age of the sample is calculated from the measured $^{40}Ar/^{39}Ar$ ratio after determining the fraction of ^{39}K converted to ^{39}Ar by analyzing the monitor mineral. Corrections for interfering Ar isotopes produced from K and Ca and for atmospheric Ar were also made.

PALEOMAGNETIC AND RADIOMETRIC RESULTS

Twenty-seven lava flows were identified in corehole {014} from the physical logging of the core. The flows range in thickness from 12' to 311'. Some sequences are composed of many lava flow units, in one case as many as 27. Sediment interbeds are uncommon in core {014} and, when present, range in thickness from 1' to 12'. Basaltic lava flows of the Snake River Plain are similar to one another in terms of general petrographic characteristics. Flows in this cored section are more phyric than flows in cores studied earlier. This was useful in deciding flow boundaries. Detailed core descriptions will be presented in a future report.

Paleomagnetic measurements

Paleomagnetic measurements, specifically inclination and intensity, were made on 396 samples in corehole {014}. Samples have both normal and reversed magnetic polarity and yielded flow-averaged inclinations ranging from +47.0° to +74.3°, and from -41.0° to -63.9° (Figure 2; Table 1). Error envelopes about these mean inclinations are small (~2°), except for

flow 23, from which too few specimens could be taken due to poor core recovery. This particular occurrence was caused by loss of the hole at 1767' due to rubble, which caused the drill string to bind. The hole was grouted with the drill rods in place, unfortunately trapping them and filled the hole with more than 1000' of concrete. The hole was then redrilled back to the original level and coring began again, encountering the lithologically and paleomagnetically distinct flow #24. Presumably, loss of the hole was caused by rubble located at the base of flow #23.

The magnetic polarity variation over the 1910' length of core {014} follows the expected pattern of normal polarity over reversed polarity, with the boundary between the layers at 923' depths. The usual assumption is that this boundary is the base of the Brunhes Chronozone, and the top of the Matuyama Chronozone. However, $^{40}Ar/^{39}Ar$ data presented later will indicate that this is not the case in this well. An additional normal-polarity flow (#27) is found near the base of the core, at 1890'. The core bottomed at 1910' in this normal-polarity flow. Considering its great depth, this flow could represent the Olduvai Subchronozone, or possibly the top of the Gauss Chronozone.

Paleomagnetic measurements have also been made on 66 samples from corehole DH-50 at a potential facility location east of the ANL-West facilities, and about 1 1/4 mile east of corehole {014}. The 252'-long core from DH-50 cuts 4 flows, and possibly bottoms in a fifth (Table 2) These flows all have normal magnetic polarity, generally steep inclination values, and have typically small (~2°) error envelopes.

A significant degree of paleomagnetic correlation can be found between flows of the two cored sections, and with the uppermost lava flows at the surface as mapped and described by Kuntz and others (1994). Flow #1 having mean inclination values of 65.8°±1.0°{014}, and 65.5°±1.2°{DH-50}, correlates well with the mean inclination value of 66.1° from site 4B691 taken in flows of Microwave Butte along Hwy 20. This is the lava field into which both wells spud and, though it has not been dated, it is known to overlie flows with a K-Ar age of 233 ± 34 ka (Champion and others, 1988). Flow #3 having mean inclinations of 69.3°± 1.1°{014}, and

70.7°±1.3°{DH-50}, and flow #4 with values of 70.2°±2.7°{014} and 68.6°±2.4°{DH-50}, also correlate well. Flow #3 is composed of multiple flow units, whereas flow #4 is a single, thick flow unit. Correlation of flow #3 with the flows of Radio Facility Butte, which have the same petrographic characteristics and a mean inclination value of 69.6° from site 4B811 taken near the vent, seems strong. Radio Facility Butte has a K-Ar age of 358±46 ka (Kuntz and others, 1994). Flow #2 in {DH-50}, having a mean inclination value of 65.5°±3.9°, does not correlate well with flow #2 in {014}, which has a steeper inclination value of 74.3°±2.3°, but the inclination of flow #2 in {DH-50} is similar to the mean inclination of 64.5° from site 4B739 taken in lava flows of Deuce Butte along Hwy 20. Samples of coreholes located directly adjacent to {DH-50}, and from the same footage interval as flow #2 produced a mean K-Ar age of 325±45 ka (Kuntz and Dalrymple, 1979), thus we believe this age applies to Deuce Butte. Flow #2 in well {014} may correlate to flows which outcrop north and northeast of Argonne National Laboratory-West. However, there is no surface paleomagnetic data from these flows, and the older flows have been buried by the very extensive flows from Microwave Butte.

$^{40}Ar/^{39}Ar$ measurements

Ages were measured on five samples of basalt from {014}. After petrographic examination samples from depths of 470', 897', 1263', 1733', and 1878' from flows 8, 11, 16, 22, and 26, respectively, were chosen for $^{40}Ar/^{39}Ar$ analysis.

$^{40}Ar/^{39}Ar$ incremental-heating experiments were made on splits of approximately 100 mg of sample material sized to 1/2 to 1 mm. The resistance-heated furnace used to extract Ar is attached to the cleanup system and mass spectrometer described by Dalrymple (1989). The furnace is modified from the design of Staudacher and others (1978). Heating temperatures were controlled with an optical fiber thermometer.

In an incremental-heating experiment, the sample is heated to a given temperature and an apparent age is calculated for the gas extracted at that temperature. In calculating an apparent age, it is assumed that the non-radiogenic Ar in a sample is atmospheric in isotopic composition. Analytical data are given in Table 3. The data from incremental-heating experiments are

commonly displayed as either an age spectrum diagram, or an isotope correlation or isochron diagram. Examples of these diagrams are shown as Figures 3 through 12. For the age spectrum, an apparent age is calculated for each gas fraction after corrections are made for interfering Ar isotopes produced in the reactor, and the results plotted on an age spectrum diagram with apparent age on the ordinate and cumulative percentage of ^{39}Ar released on the abscissa. The spectrum description (Table 4) is a subjective assessment of the quality of a plateau. The ages of gas increments on a good plateau agree better than the increments on a fair plateau, and the percent of ^{39}Ar producing a good plateau is higher than the percent of ^{39}Ar producing a fair plateau. For the isochron diagram (Merrihue and Turner, 1966), $^{40}Ar/^{36}Ar$ is plotted on the ordinate and $^{39}Ar/^{36}Ar$ on the abscissa . The slope of the isochron is $^{40}Ar_r/^{39}Ar_K$ (where subscripts r=radiogenic and K=potassium-derived) from which the age is calculated. The intercept on the ordinate gives the $^{40}Ar/^{36}Ar$ ratio of the non-radiogenic or trapped Ar; this isotopic composition usually is atmospheric for terrestrial samples. Some workers use another correlation diagram, called the inverse diagram, which is a plot of $^{36}Ar/^{40}Ar$ vs. $^{39}Ar/^{40}Ar$. In this diagram the intercept on the abscissa is the inverse of the ratio $^{40}Ar_r/^{39}Ar_K$ and the intercept on the ordinate is the composition of the trapped (atmospheric) Ar. The two types of correlation diagrams yield the same information provided the correct mathematics are used for estimating correlation coefficients and for the least squares fit (Dalrymple and others, 1988).

Generally accepted criteria for a meaningful incremental heating age are: (1) well-defined plateau (horizontal age spectrum) for more than 50 percent of the ^{39}Ar released; (2) well-defined isochron for the plateau gas fractions; (3) concordant plateau and isochron ages; and (4) $^{40}Ar/^{36}Ar$ isochron intercept not significantly different from 295.5 (Lanphere and Dalrymple, 1978).

ANL-470: Basalt from flow 8 has a fair plateau containing 86% of the ^{39}Ar released; the weighted mean plateau age is 489 ± 10 ka (Fig. 3). The six gas increments that constitute the plateau have monotonically decreasing ages with increasing temperature. The $^{40}Ar/^{39}Ar$ intercepts of the isochrons agree with the atmospheric value within analytical uncertainty (Fig.

4). However, the intercept values of about 291 suggest that the calculated ages of the plateau gas increments may be too young. Therefore, the preferred age of ANL-470 is the isochron age of 565 ± 94 ka.

ANL-897: Basalt from flow 11 has a good plateau containing 98% of the ^{39}Ar released (Fig. 5). The weighted mean plateau age of 1.151 ± 0.015 Ma is in excellent agreement with the isochron age of 1.170 ± 0.051 Ma and the inverse age of 1.171 ± 0.050 Ma (Fig. 6). The intercepts of the isochron are in good agreement with the atmospheric composition. The age for flow 11 was somewhat older than expected. The upper 11 flows in well {014} are normally magnetized, and it was assumed that these flows constituted a thick section of basalt erupted during the Brunhes Chron. However, the $^{40}Ar/^{39}Ar$ results indicate that flow 11 was erupted during the Cobb Mountain Subchron (Mankinen and others, 1978), and that there was a major slowdown or hiatus in eruptive activity between eruption of flows 8 and 11. Turrin and others (1994) reported an age of 1.186 ± 0.006 Ma for sanidine from the rhyolite of Alder Creek, the type locality for the Cobb Mountain Subchron. Measurements on this sanidine in the Menlo Park laboratory have a larger scatter than is desirable, but the mean $^{40}Ar/^{39}Ar$ age and standard deviation for 16 measurements are 1.150 ± 0.014 Ma. The preferred age for ANL-897 is 1.15 Ma.

ANL-1263: Basalt from flow 16 yielded a complex set of results. The initial data reduction produced a fair plateau containing 55% of the ^{39}Ar released and a weighted mean plateau age of 1.404 ± 0.039 Ma. However, the isochron and inverse ages of 1.211 ± 0.102 Ma and 1.211 ± 0.101 Ma, respectively, do not agree with the plateau age within analytical uncertainties. In addition, the intercept of the isochron is 302.7 ± 3.7 and does not agree with the atmospheric value, meaning that the assumption used in calculating the ages of individual increments has not been met. The ages of gas increments were recalculated using an $^{40}Ar/^{36}Ar$ ratio of 302.7 for non-radiogenic Ar. The recalculated ages produced a fair plateau containing 55% of the ^{39}Ar released and a weighted mean plateau age of 1.207 ± 0.039 Ma (Fig. 7). The isochron and inverse ages of 1.203 ± 0.236 Ma and 1.203 ± 0.235 Ma, respectively, agree with

the plateau age (Fig. 8). The intercept of the isochron has a value of 295.6 which is the atmospheric value. Thus, the preferred age of ANL-1263 is 1.21 Ma.

ANL-1733: Basalt from flow 22 has a fair plateau containing 50% of the ^{39}Ar released (Fig. 9). The plateau age is based on Ar extracted between 550° and 1000° with the 600°, 650°, and 700° increments not included, because they do not fall on isochron. The weighted mean plateau age is 1.441 ± 0.042 Ma and is in good agreement with the isochron and inverse ages of 1.453 ± 0.061 Ma and 1.453 ± 0.061, respectively (Fig. 10). The intercept of the isochron has a value of 295.2 ± 1.1 in good agreement with the atmospheric value. The preferred age of ANL-1733 is 1.44 Ma.

ANL-1878: Basalt from flow 26 has a disturbed age spectrum, and it is not possible to draw a plateau on an age spectrum diagram (Fig. 11). There is a pseudoplateau at about 1.35 Ma for about 45% of the ^{39}Ar released between 640° and 850°, but this age is inconsistent stratigraphically with the age of ANL-1733. There also is a poorly-defined plateau at about 2 Ma for gas released above 900°. The overall pattern of ages might result from recoil of ^{39}Ar during irradiation because the rock is very fine-grained. If redistribution of Ar isotopes by recoil took place, then the recalculated total-fusion age is the best estimate of the age of ANL-1878. Flow 27 from a depth of 1890' to the bottom of {014} at 1910' has normal magnetic polarity. It is likely this flow was erupted during the Olduvai Subchron which has boundary ages of 1.77 Ma and 1.98 Ma (Cande and Kent, 1995). The recalculated total-fusion age of ANL-1878 is 1.75 Ma and is consistent with assigning an Olduvai age to flow 27.

DISCUSSION

$^{40}Ar/^{39}Ar$ ages and paleomagnetic inclination determinations document that 27 lava flows were encountered in core ANL-OBS-AQ-014, and that ages of the lava flows decrease monotonically with ascending stratigraphic order. In addition, the magnetic polarity of the lava flows is consistent with the geomagnetic polarity timescale as presently understood (Cande and Kent, 1995). Figure 13 is a graph of lava flow age vs. depth for well {014}, plotted such that ages are applied to the top footage of a lava flow as defined by the paleoinclination work, and not

at the exact footage of the argon sample. Each data point can then be read to indicate that the stack of flows accumulated to some depth footage at a given time. This rate of accumulation of the basalt sections through time is remarkably uniform in most INEEL wells.

Unlike other INEEL wells though, which are generally shorter in length, the accumulation rate of lava flows in well {014} is, at times, highly irregular. For lava flows #2 through #8, more than 500' of flow units accumulated in a little more than 200 k.y. This interval is followed by the accumulation of only two more flows (#1 and #2) in the ensuing 358 k.y., suggesting that the Argonne-West facility is currently enjoying a hiatus of lava accumulation, and a relatively decreased volcanic hazard, as is the rest of the southcentral and southeastern parts of INEEL. Also flow #11 has an age of 1.15 Ma, and only 50' of lava accumulation comprises flows #9 and #10. It is clear that the flow #2 through #8 interval is preceded by very slow lava accumulation, or a possible hiatus of nearly 600 k.y.

Deeper levels of well {014} also show fast and probably nonuniform rates of lava accumulation. From the top of flow #11 at 612', dated at 1.15 Ma, through the 1.21 Ma age of flow #16, to the base of flow #22 at 1754', emplaced at 1.44 Ma, accumulation of almost 1150' of lava flow units required slightly less than 300 k.y. The data suggest average rates of accumulation of 3000'/m.y. over this interval. The poorly-determined, integrated-gas age of 1.75 Ma from the sample from flow #26, and the probable identification of the Olduvai Subchronozone in flow #27, suggest that the accumulation of 144' of flow units in flows #26 through #23 took over 300 k.y. at a very low average rate. Alternatively, a hiatus of several hundred k.y. duration may exist between two of these deep flows.

The analysis of the variable accumulation rates of core {014} as presented here could change considerably if additional age measurements were available. Clearly, additional age experiments in the footage intervals near the purported hiatuses, and within the rapid accumulation intervals, would sharpen our understanding of the nature of the lava flow accumulation process, and resulting volcanic hazard, at the location of the Argonne Laboratory West Facilities.

ACKNOWLEDGEMENTS

$^{40}Ar/^{39}Ar$ sample preparation, encapsulation, and mass spectrometry was assisted by James Saburomaru and Forest McFarland. The manuscript was reviewed by Mel Kuntz and Mike McCurry. Creation of the deep Argonne corehole was made possible by the perseverance of Chris Martin of the Argonne National Laboratory, and we all owe him a considerable debt. Consultations with Mel Kuntz regarding the physical stratigraphy and petrography of core ANL-OBS-AQ-014 were critical to the evaluation of that core. Discussions with Steve Anderson were valuable a priori elements of this study. Chemical data on a key lava flow were graciously shared by Mike McCurry and Lee Morse of Idaho State University. Funding from the Idaho Universities Consortium of the Idaho Water Resource Research Institute made it possible to carry out this research project.

REFERENCES

Cande, S.C., and Kent, D.V., 1995, Revised calibration of the geomagnetic polarity timescale for the Late Cretaceous and Cenozoic: Journal of Geophysical Research, v. 100, p. 6093-6095.

Champion, D.E., Lanphere, M.A., and Kuntz, M.A., 1988, Evidence for a new geomagnetic reversal from lava flows in Idaho: Discussion of short polarity reversals in the Brunhes and late Matuyama polarity chrons: Journal of Geophysical Research, v. 93, p. 11,667-11,680.

Dalrymple, G.B., 1989, The GLM continuous laser system for $^{40}Ar/^{39}Ar$ dating: Description and performance characteristics, U.S. Geological Survey Bulletin 1890, p. 89-96.

Dalrymple, G.B., and Lanphere, M.A., 1969, Potassium-Argon Dating: W.H. Freeman, New York, 258 pp.

Dalrymple, G.B., Lanphere, M.A., and Pringle, M.P., 1988, Correlation diagrams in $^{40}Ar/^{39}Ar$ dating: is there a correct choice?: Geophysical Research Letters, v. 15, p. 589-591.

Kuntz, M.A., and Dalrymple, G.B., 1979, Geology, geochronology, and potential volcanic hazards in the Lava Ridge-Hells Half Acre area, eastern Snake River Plain, Idaho: U.S. Geological Survey Open-File Report 79-1657, 66p.

Kuntz, M.A., Skipp, Betty, Lanphere, M.A., Scott, W.E., Pierce, K.L., Dalrymple, G.B., Champion, D.E., Embree, G.F., Page, W.R., Morgan, L.A., Smith, R.P., Hackett, W.R., and Rodgers, D.W., 1994, Geologic Map of the Idaho National Engineering Laboratory and adjoining areas, eastern Idaho: U.S. Geological Survey Miscellaneous Investigations Map I-2330, scale 1:100,000.

Lanphere, M.A., and Dalrymple, G.B., 1978, The use of $^{40}Ar/^{39}Ar$ data in evaluation of disturbed K-Ar systems: U.S. Geological Survey Open-File Report 78-701, p. 241-243.

Mankinen, E.A., and Dalrymple, G.B., 1972, Electron microprobe evaluation of terrestrial basalts for whole-rock dating: Earth and Planetary Science Letters, v. 17, p. 159-168.

Mankinen, E.A., Donnelly, J.M., Grommé, C.S., 1978, Geomagnetic polarity event recorded at 1.1 m.y. on Cobb Mountain, Clear Lake volcanic field, California: Geology, v. 6, p. 653-656

Merrihue, C., and Turner, G., 1966, Potassium-argon dating by activation with fast neutrons: Journal of Geophysical Research, v. 71, p. 2852-2857.

Staudacher, Th, Jessberger, E.K., Dörflinger, D., and Kiko, J., 1978, A refined ultrahigh-vacuum furnace for rare gas analysis: Journal of Physics E Scientific Instruments, v. 11, p. 781-784.

Turrin, B.D., Donnelly-Nolan, J.M., and Hearn, B.C., Jr., 1994, $^{40}Ar/^{39}Ar$ ages from the rhyolite of Alder Creek, California: Age of the Cobb Mountain Normal-Polarity Subchron revisited: Geology, v. 22, p.251-254.

FIGURE CAPTIONS

Figure 1. Location map showing the boundary of the Idaho National Engineering and Environmental Laboratory, certain facilities areas, and the location of corehole ANL-OBS-AQ-014.

Figure 2. Plot of core stratigraphy, mean paleomagnetic inclination value, and 40Ar/39Ar ages in top (a) and bottom (b) portions of well ANL-OBS-AQ-014. Diagonal ruling indicates sedimentary interbeds, horizontal lines are flow contacts, solid(open) points represent normal(reversed) polarity data for individual samples, and light stippling pattern represents 95% confidence limits around the mean inclination values.

Figure 3. Age spectrum diagram for sample ANL-470 from corehole ANL-OBS-AQ-014.

Figure 4. Isochron and inverse isochron diagram for sample ANL-470 from corehole ANL-OBS-AQ-014

Figure 5. Age spectrum diagram for sample ANL-897 from corehole ANL-OBS-AQ-014.

Figure 6. Isochron and inverse isochron diagram for sample ANL-897 from corehole ANL-OBS-AQ-014

Figure 7. Age spectrum diagram for sample ANL-1263 from corehole ANL-OBS-AQ-014.

Figure 8. Isochron and inverse isochron diagram for sample ANL-1263 from corehole ANL-OBS-AQ-014

Figure 9. Age spectrum diagram for sample ANL-1733 from corehole ANL-OBS-AQ-014.

Figure 10. Isochron and inverse isochron diagram for sample ANL-1733 from corehole ANL-OBS-AQ-014

Figure 11. Age spectrum diagram for sample ANL-1878 from corehole ANL-OBS-AQ-014.

Figure 12. Isochron and inverse isochron diagram for sample ANL-1878 from corehole ANL-OBS-AQ-014

Figure 13. Graph of lava flow age plotted against depth for well ANL-OBS-AQ-014, showing nonuniform accumulation rate of lava flows near Argonne National Laboratory-West for the past approx. 1.8 Ma. Very rapid accumulation is followed by hiatus, sometimes lasting on the order of 500 k.y.

Table 1. Lithology, polarity, inclination and depth data for well ANL-OBS-AQ-014

Basalt flow	Inclination	Depth Range
1	+65.8°±1.0°	1'-50'
[sediment]		50'-51'
2	+74.3°±2.3°	51'-63'
3	+69.3°±1.1°	63'-178'
[unrecovered core]		178'-181'
4	+70.2°±2.7°	181'-261'
5	+65.0°±1.2°	261'-371'
6	+66.4°±2.3°	371'-400'
7	+55.4°±2.0°	400'-440'
8	+47.0°±1.5°	440'-562'
9	+57.6°±3.0°	562'-582'
[sediment]		582'-583'
10	+53.4°±3.5°	583'-605'
[sediment]		605'-612'
11	+58.4°±1.0°	612'-923'
12	-47.7°±1.5°	923'-1047'
13	-41.1°±2.3°	1047'-1095'
14	-54.4°±1.3°	1095'-1153'
15	-53.7°±2.5°	1153'-1194'
[sediment]		1194'-1205'
16	-57.1°±1.0°	1205'-1353'
17	-50.8°±1.8°	1353'-1396'
18	-41.0°±2.3°	1396'-1439'
19	-42.4°±1.1°	1439'-1474'
[sediment]		1474'-1475'
20	-50.8°±1.4°	1475'-1595'
21	-61.2°±2.8°	1595'-1634'
22	-63.9°±1.2°	1634'-1754'
23	-58.1°±15.5°	1754'-1767'
24	-63.7°±2.1°	1760'-1781'
[sediment]		1781'-1786'
25	-56.1°±2.2°	1786'-1841'
[sediment]		1841'-1853'
26	-52.8°±5.9°	1853'-1882'
[sediment]		1882'-1890'
27	+56.8°±1.5°	1890'-1910'

Table 2. Lithology, polarity, inclination and depth data for well DH-50

Basalt flow	Inclination	Depth Range
[sediment]		0'-8'
1	+65.5°±1.2°	8-68'
[sediment]		68'-73'
2	+65.5°±3.9°	73'-88'
[sediment]		88'-105'
3	+70.7°±1.3°	105'-183'
4	+68.6°±2.4°	183'-252'

TABLE 3: $^{40}Ar/^{39}Ar$ analytical data for basalt samples ANL-OBS-AQ-014 corehole, Idaho National Engineering and Environmental Laboratory, Idaho

ANL-470 [J=0.00037958]

plateau age=0.489 ±0.010 Ma; isochron age=0.565 ± 0.094 Ma; inverse age=0.564 ±0.089 Ma; total gas age=0.475 ±0.011 Ma

Temp (°C)	$^{40}Ar/^{39}Ar$	$^{37}Ar/^{39}Ar$	$^{36}Ar/^{39}Ar$	Moles $^{40}Ar_{rad}$	$^{40}Ar_{rad}$ (%)	$^{39}Ar_{Ca}$ (%)	$^{36}Ar_{Ca}$ (%)	K/Ca	^{39}Ar (%)	Age (Ma)	± s.d.
450	129.560	6.337	0.4245	4.283E-16	3.6	0.45	0.4	0.077	0.0	3.18	± 2.89
500	14.403	3.105	0.04637	9.160E-15	6.6	0.22	1.9	0.157	4.9	0.655	± 0.042
550	10.162	2.925	0.03243	1.941E-14	8.1	0.21	2.5	0.167	12.0	0.563	± 0.028
600	8.459	2.847	0.02675	2.794E-14	9.4	0.20	3.0	0.172	18.0	0.541	± 0.023
650	6.771	2.910	0.02122	2.797E-14	11.0	0.21	3.9	0.168	19.2	0.509	± 0.019
700	6.884	3.167	0.02189	2.592E-14	9.9	0.22	4.1	0.154	19.4	0.465	± 0.019
750	9.662	3.647	0.03175	1.236E-14	6.0	0.26	3.2	0.134	10.8	0.399	± 0.027
800	16.224	3.744	0.05419	6.512E-15	3.2	0.26	1.9	0.131	6.4	0.357	± 0.046
850	26.480	2.800	0.08944	2.987E-15	1.1	0.20	0.9	0.175	5.4	0.194	± 0.074
900	30.390	5.819	0.10295	3.572E-15	1.5	0.41	1.6	0.084	4.0	0.311	± 0.086

ANL-897 [J=0.00038586]

plateau age=1.151 ± 0.015 Ma; isochron age=1.170 ± 0.0.051 Ma; inverse age=1.171 ± 0.050 Ma; total gas age=1.211 ± 0.019 Ma

Temp (°C)	$^{40}Ar/^{39}Ar$	$^{37}Ar/^{39}Ar$	$^{36}Ar/^{39}Ar$	Moles $^{40}Ar_{rad}$	$^{40}Ar_{rad}$ (%)	$^{39}Ar_{Ca}$ (%)	$^{36}Ar_{Ca}$ (%)	K/Ca	^{39}Ar (%	Age (Ma)	± s.d.
450	99.83	3.024	0.3257	1.113E-16	3.8	0.21	0.3	0.162	0.0	2.67	± 8.76
500	15.088	8.637	0.04783	6.062E-15	11.1	0.61	5.1	0.056	4.4	1.170	± 0.075
550	10.413	8.025	0.03169	1.953E-14	16.5	0.57	7.1	0.061	13.8	1.199	± 0.035
600	8.724	7.209	0.02604	3.108E-14	18.7	0.51	7.8	0.068	23.1	1.139	± 0.028
650	7.759	6.777	0.02226	2.454E-14	22.5	0.48	8.6	0.072	17.0	1.219	± 0.028
700	9.570	6.908	0.02924	1.889E-14	15.7	0.49	6.6	0.071	15.2	1.050	± 0.032
750	14.010	6.731	0.04361	1.074E-14	12.0	0.48	4.3	0.072	7.7	1.175	± 0.051

800	21.62	5.330	0.06899	7.297E-15	7.8	0.38	2.2	0.092	5.3	1.170	± 0.075
850	28.79	4.272	0.09494	2.773E-15	3.8	0.30	1.3	0.114	3.1	0.760	± 0.115
950	33.91	5.846	0.11116	4.669E-15	4.6	0.41	1.5	0.083	3.6	1.084	± 0.113
1050	64.87	72.30	0.2332	7.533E-15	3.0	5.1	8.7	0.0064	4.4	1.443	± 0.245
1150	36.02	95.74	0.13531	3.462E-15	11.1	6.8	19.9	0.0048	1.0	2.97	± 0.35
1300	37.17	73.29	0.12775	6.582E-15	14.8	5.2	16.1	0.0063	1.4	4.04	± 0.27

ANL-1263 **[J=0.00036724]**

plateau age=1.207 ± 0.039; isochron age=1.203 ± 0.100 Ma; inverse age=1.203 ± 0.099 Ma; total gas age=1.002 ± 0.036 Ma

Temp (°C)	$^{40}Ar/^{39}Ar$	$^{37}Ar/^{39}Ar$	$^{36}Ar/^{39}Ar$	Moles $^{40}Ar_{rad}$	$^{40}Ar_{rad}$ (%)	$^{39}Ar_{Ca}$ (%)	$^{36}Ar_{Ca}$ (%)	K/Ca	^{39}Ar (%	Age (Ma)	± s.d.
450	235.6	59.37	0.3289	1.035E-15	60.8	4.2	5.1	0.0079	0.0	96.50	± 61.90
500	20.13	14.129	0.06780	1.622E-15	6.3	1.00	5.9	0.034	3.5	0.851	± 0.273
550	11.583	13.388	0.03799	1.124E-14	12.7	0.95	9.9	0.036	20.8	0.983	± 0.057
600	12.152	15.396	0.03931	1.565E-14	14.9	1.1	11.0	0.031	23.4	1.215	± 0.056
650	14.176	18.101	0.04709	1.160E-14	12.4	1.3	10.8	0.027	17.8	1.184	± 0.070
700	17.099	19.906	0.05730	9.656E-15	10.6	1.4	9.8	0.024	14.3	1.223	± 0.084
750	25.21	21.11	0.08696	4.756E-15	5.0	1.5	6.8	0.023	10.1	0.853	± 0.116
800	42.53	19.925	0.14733	1.211E-15	1.5	1.4	3.8	0.024	5.0	0.437	± 0.214
900	79.18	13.983	0.2747	-1.553E-15	-1.0	0.99	1.4	0.035	5.1	-.550	± 0.264

ANL-1733 **[J=0.00035232]**

plateau age=1.441 ± 0.042 Ma; isochron age=1.453 ± 0.061 Ma; inverse age=1.453 ± 0.061; total gas age=1.443 ± 0.223 Ma

Temp (°C)	$^{40}Ar/^{39}Ar$	$^{37}Ar/^{39}Ar$	$^{36}Ar/^{39}Ar$	Moles $^{40}Ar_{rad}$	$^{40}Ar_{rad}$ (%)	$^{39}Ar_{Ca}$ (%)	$^{36}Ar_{Ca}$ (%)	K/Ca	^{39}Ar (%	Age (Ma)	± s.d.
450	6296.5	209.8	20.14	7.544E-15	5.8	14.8	0.3	0.0020	0.0	252.8	± 474.5
500	133.32	10.532	0.4499	4.918E-16	0.9	0.74	0.7	0.046	0.9	0.801	± 0.991
550	23.73	10.744	0.07557	7.617E-15	9.7	0.76	4.0	0.045	7.6	1.467	± 0.111

600	11.235	10.977	0.03496	1.301E-14	16.2	0.78	8.8	0.044	16.3	1.163	± 0.054
650	8.487	9.052	0.02452	1.628E-14	23.5	0.64	10.4	0.054	18.6	1.275	± 0.046
700	8.668	6.443	0.02434	1.225E-14	23.2	0.45	7.4	0.076	13.9	1.283	± 0.056
750	10.586	5.822	0.02951	1.195E-14	22.2	0.41	5.5	0.084	11.6	1.499	± 0.067
800	16.043	5.096	0.04816	9.317E-15	13.9	0.36	3.0	0.096	9.5	1.424	± 0.084
850	27.38	4.430	0.08734	5.879E-15	7.1	0.31	1.4	0.110	6.9	1.238	± 0.122
950	37.20	3.817	0.11926	8.031E-15	6.1	0.27	0.9	0.128	8.1	1.448	± 0.122
1000	92.80	20.81	0.3121	6.688E-15	2.5	1.5	1.9	0.023	6.5	1.488	± 0.246

ANL-1878 **[J=0.00036712]**

total gas age=1.753 ± 0.039 Ma

Temp (°C)	$^{40}Ar/^{39}Ar$	$^{37}Ar/^{39}Ar$	$^{36}Ar/^{39}Ar$	Moles $^{40}Ar_{rad}$	$^{40}Ar_{rad}$ (%)	$^{39}Ar_{Ca}$ (%)	$^{36}Ar_{Ca}$ (%)	K/Ca	^{39}Ar (%	Age (Ma)	± s.d.
450	8580.2	0.14347	28.51	1.145E-14	1.8	0.010	0.000	3.42	0.0	100.32	± 268.0
500	1750.3	0.9401	5.945	-2.762E-15	-0.4	0.066	0.004	0.521	0.1	4.25	± 10.55
550	180.50	0.13036	0.5892	2.335E-14	3.6	0.009	0.006	3.76	0.6	4.24	± 0.48
600	42.92	0.17501	0.12369	1.072E-13	14.9	0.012	0.040	2.80	2.6	4.22	± 0.11
625	28.41	0.19549	0.09086	4.866E-14	5.6	0.014	0.060	2.51	4.8	1.047	± 0.075
640	18.623	0.18326	0.05623	6.219E-14	10.9	0.013	0.092	2.67	4.8	1.339	± 0.048
655	11.775	0.18838	0.03312	5.095E-14	17.0	0.013	0.16	2.60	4.0	1.327	± 0.033
675	12.402	0.19330	0.03485	6.065E-14	17.1	0.014	0.16	2.53	4.5	1.404	± 0.032
700	13.605	0.2063	0.03880	7.390E-14	15.8	0.015	0.15	2.37	5.4	1.427	± 0.034
725	14.653	0.2202	0.04249	7.341E-14	14.4	0.016	0.15	2.23	5.5	1.400	± 0.037
750	15.019	0.2350	0.04363	7.150E-14	14.3	0.017	0.15	2.08	5.2	1.421	± 0.038
775	19.617	0.2501	0.05972	6.577E-14	10.1	0.018	0.12	1.96	5.2	1.317	± 0.050
800	29.24	0.2595	0.09246	5.165E-14	6.6	0.018	0.079	1.89	4.2	1.287	± 0.076
825	22.27	0.2831	0.06897	3.905E-14	8.6	0.020	0.12	1.73	3.2	1.269	± 0.058
850	24.80	0.2981	0.07685	3.631E-14	8.5	0.021	0.11	1.64	2.7	1.403	± 0.064

875	43.65	0.3261	0.14445	1.983E-14	2.3	0.023	0.063	1.50	3.1	0.658 ± 0.117
900	73.68	0.2560	0.2354	1.067E-13	5.6	0.018	0.031	1.91	4.1	2.74 ± 0.19
925	56.22	0.4349	0.17770	1.141E-13	6.7	0.031	0.069	1.13	4.8	2.48 ± 0.15
950	44.84	0.6073	0.14039	8.217E-14	7.6	0.043	0.12	0.807	3.8	2.26 ± 0.12
975	35.77	0.5192	0.11054	1.068E-13	8.8	0.037	0.13	0.943	5.3	2.09 ± 0.09
1000	30.91	0.4864	0.09333	2.243E-13	10.9	0.034	0.15	1.01	10.5	2.23 ± 0.08
1025	22.66	0.6619	0.06699	1.528E-13	12.9	0.047	0.28	0.740	8.2	1.932 ± 0.057
1050	16.927	0.8510	0.05131	4.483E-14	10.8	0.060	0.47	0.575	3.8	1.216 ± 0.043
1075	17.870	0.8742	0.05201	2.654E-14	14.4	0.062	0.47	0.560	1.6	1.704 ± 0.062
1125	23.35	0.8700	0.06949	1.605E-14	12.4	0.061	0.35	0.563	0.9	1.912 ± 0.103
1225	76.22	1.1167	0.2479	1.245E-14	4.0	0.079	0.13	0.438	0.6	2.03 ± 0.21
1325	384.5	1.1890	1.2979	1.737E-15	0.3	0.084	0.026	0.412	0.2	0.748 ± 1.037

Ratios corrected for ^{37}Ar decay (half-life=35.1 days) and ^{39}Ar decay (half-life=269 years). Subscripts: rad, radiogenic; Ca, calcium-derived. Decay constants: =0.581x10-10yr-1, =4.692x10-10yr-1.

Table 4: $^{40}Ar/^{39}Ar$ ages from the INEEL, Corehole ANL-OBS-AQ-014

Sample No.	Plateau ^{39}Ar# (%[steps])	Plateau age (Ma)	Spectrum Description	Isochron age (Ma)	Isochron Intercept
ANL-470	86[6 of 10]	0.489 ± 0.010	fair plateau	0.565 ± 0.094	292.2 ± 5.1
ANL-895	98[10 of 13]	1.151 ± 0.015	good plateau	1.170 ± 0.051	294.5 ± 2.0
ANL-1263	55[3 of 9]	1.207 ± 0.039	fair plateau	1.203 ± 0.100	295.7 ± 3.6
ANL-1733	50[6 of 11]	1.441 ± 0.042	fair plateau	1.453 ± 0.061	295.2 ± 1.1
ANL-1878			no plateau		

Plus-or-minus values are standard deviation of analytical precision (1)

% is proportion of total ^{39}Ar defining plateau. Steps are number of gas increments on plateau.

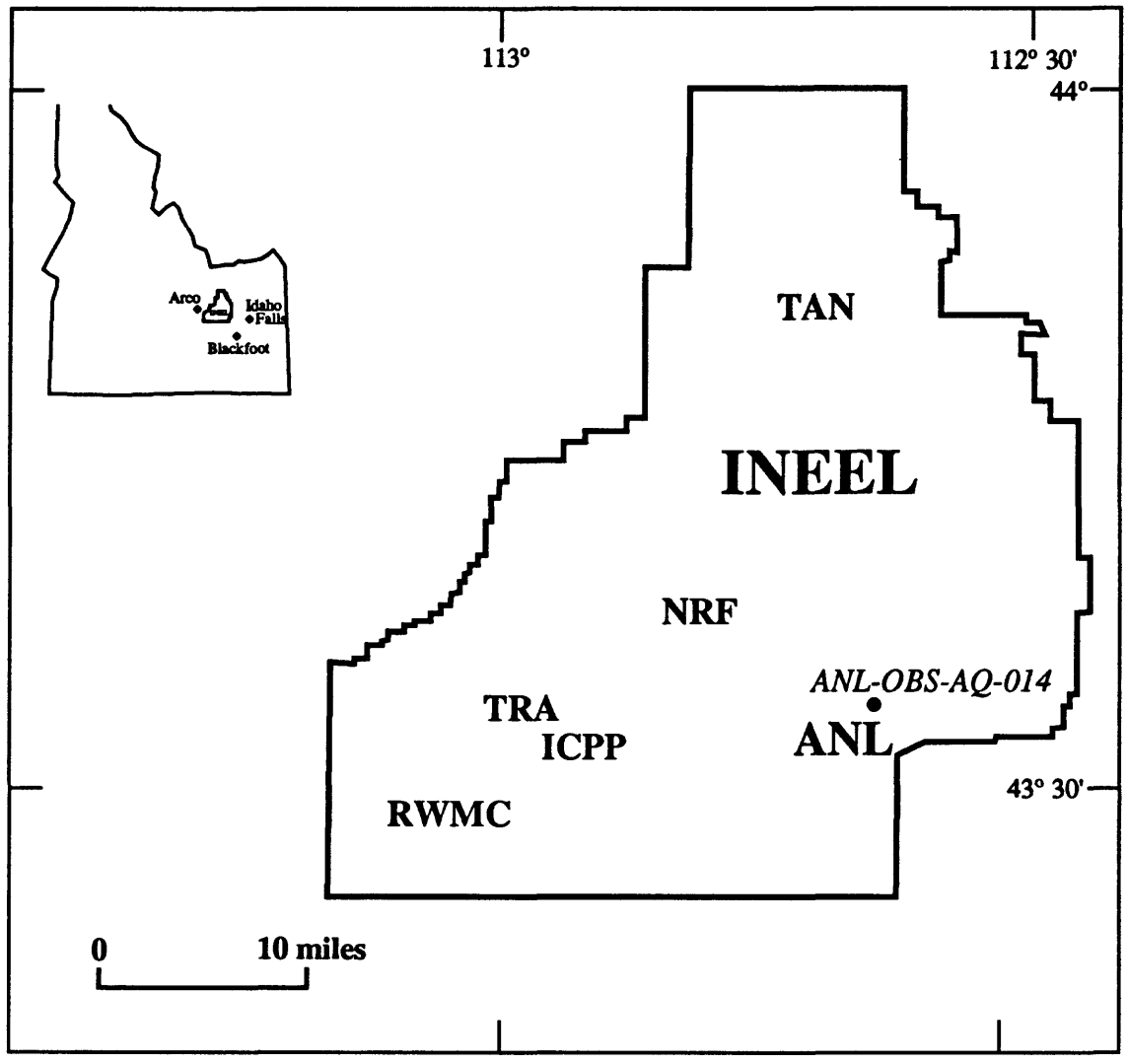

Figure 1. Location map showing the boundary of the Idaho National Engineering and Environmental Laboratory, certain facilities areas, the location of Argonne National Laboratory-West, and the position of corehole ANL-OBS-AQ-014 studied in this investigation.

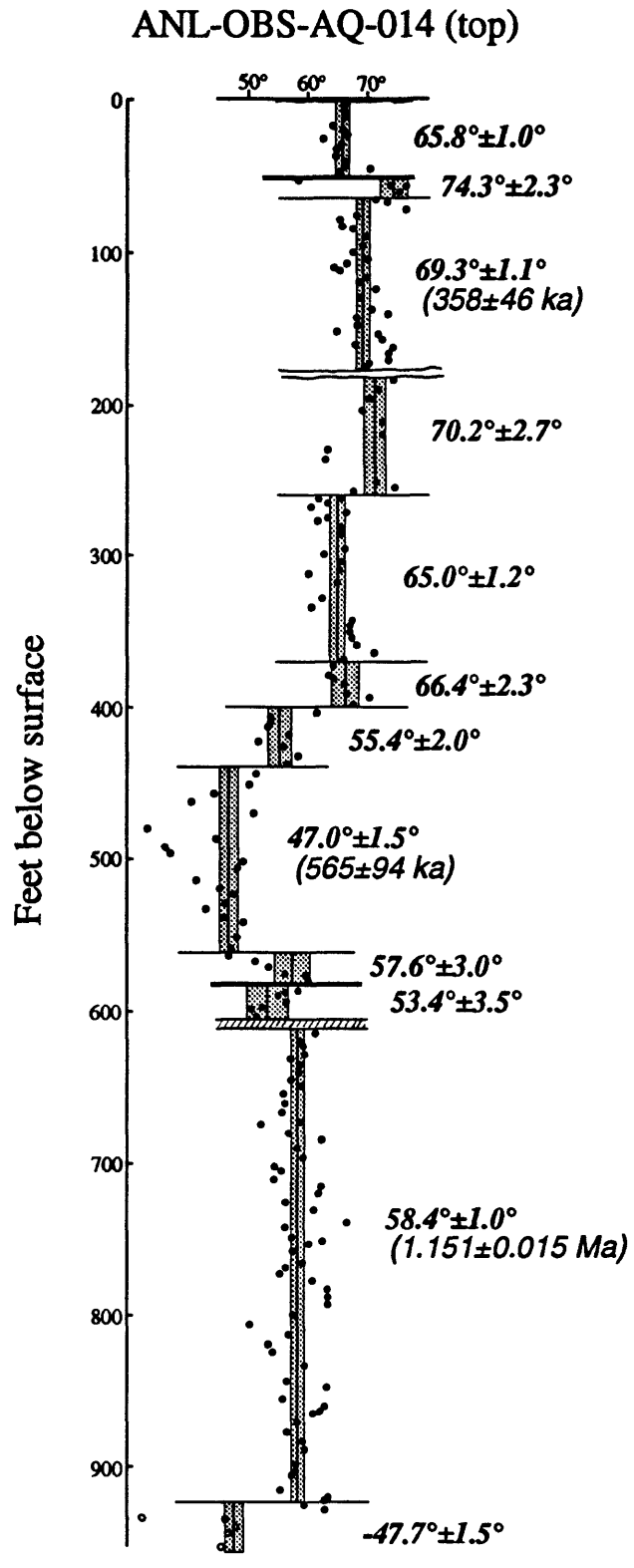

Figure 2(a) Plot of core stratigraphy, mean paleomagnetic inclination value, and 40Ar/39Ar ages in top portion of well ANL-OBS-AQ-014 at the INEEL. Diagonal ruling indicates sedimentary interbeds, horizontal lines are flow contacts, solid(open) points represent normal(reversed) polarity data for individual samples, and light stippling pattern represents 95% confidence limits around the mean inclination values.

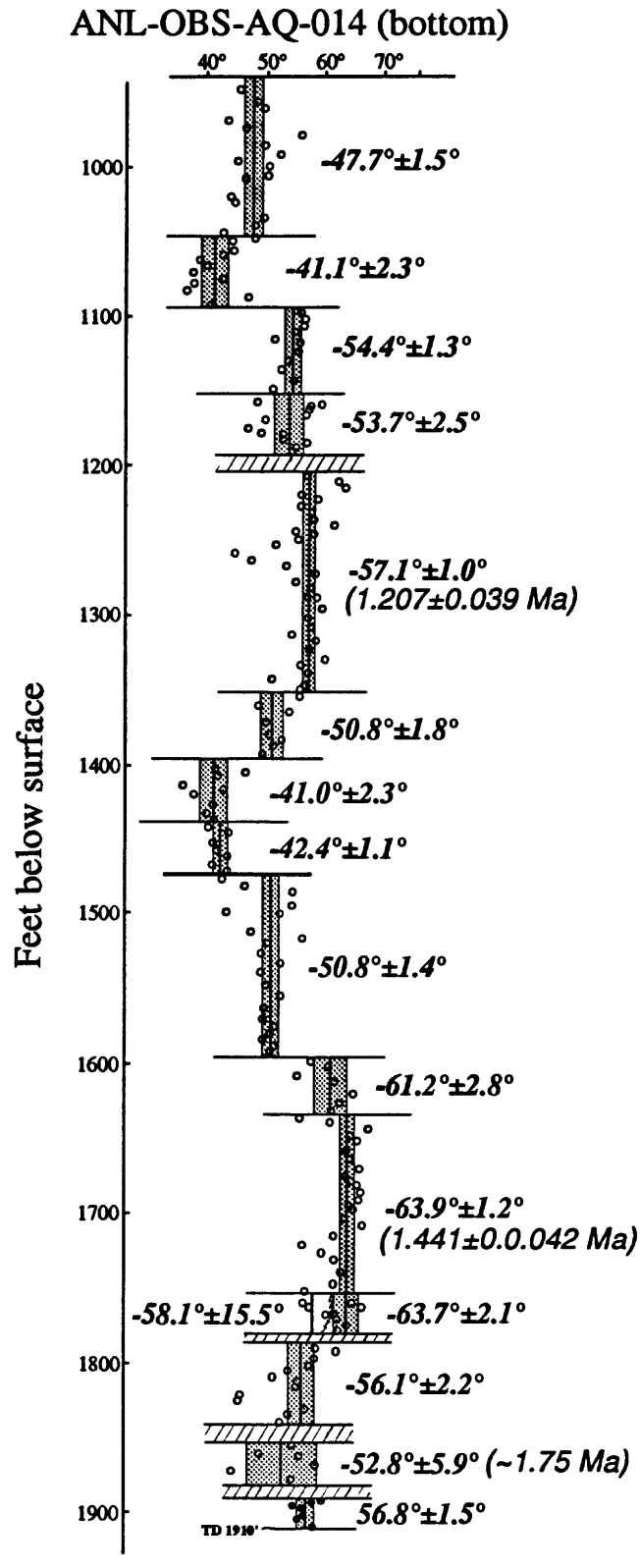

Figure 2(b) Plot of core stratigraphy, mean paleomagnetic inclination value, and 40Ar/39Ar ages in bottom portion of well ANL-OBS-AQ-014 at the INEEL. Symbols same as in Figure 2(a).

Figure 3.

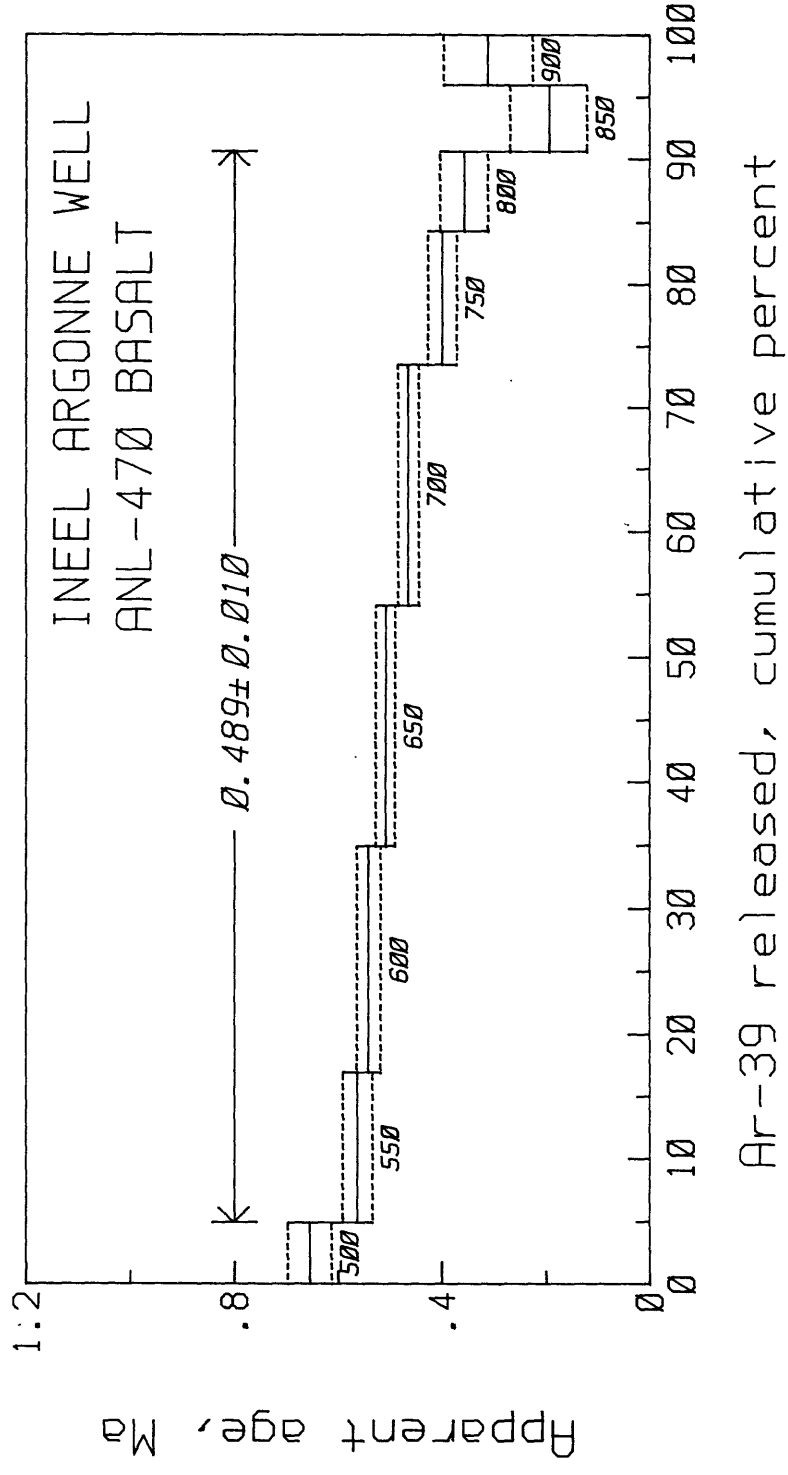
INEEL ARGONNE WELL
ANL-470 BASALT
0.489±0.010
500
550
600
650
700
750
800
850
900
1:2
.8
.4
0
0
10
20
30
40
50
60
70
80
90
100
Ar-39 released, cumulative percent
Apparent age, Ma

Figure 4.

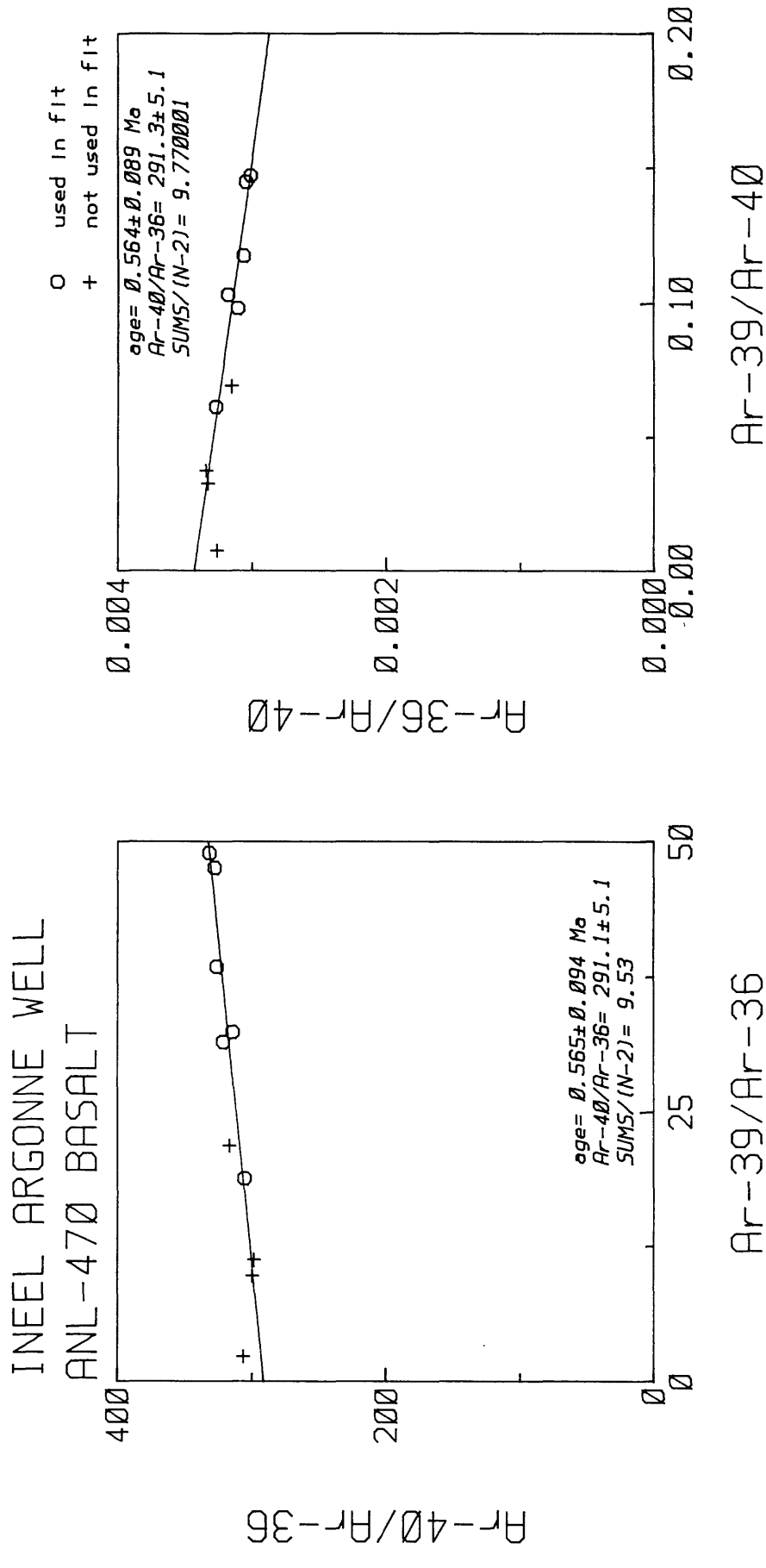
INEEL ARGONNE WELL
ANL-470 BASALT
Ar-40/Ar-36
400
200
0
0
25
50
Ar-39/Ar-36
age= 0.565± 0.094 Ma
Ar-40/Ar-36= 291.1± 5.1
SUMS/(N-2)= 9.53
Ar-36/Ar-40
0.004
0.002
0.000
0.00
0.10
0.20
Ar-39/Ar-40
o used in fit
+ not used in fit
age= 0.564± 0.089 Ma
Ar-40/Ar-36= 291.3± 5.1
SUMS/(N-2)= 9.770001

Figure 5.

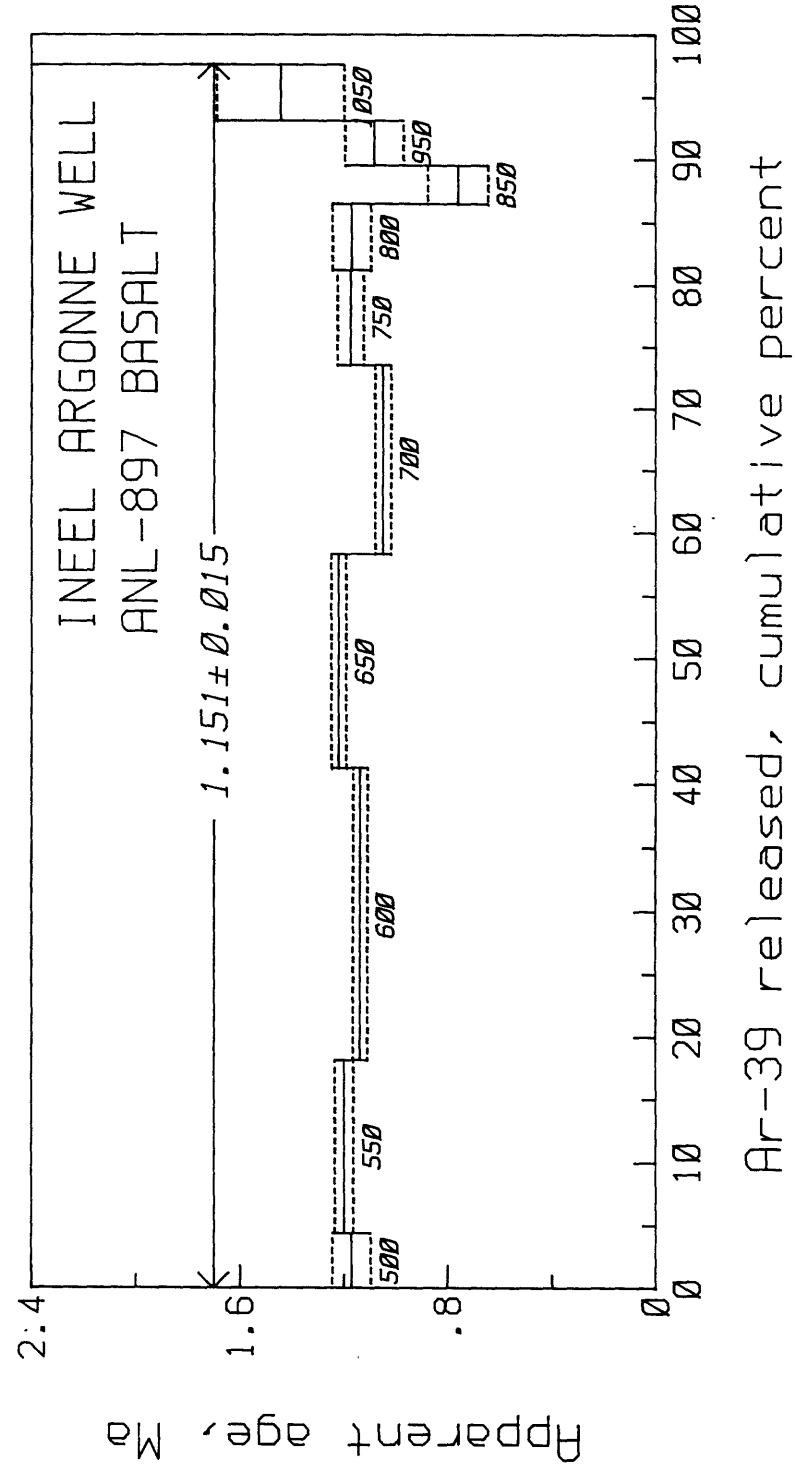
INEEL ARGONNE WELL
ANL-897 BASALT
1.151±0.015
500
550
600
650
700
750
800
850
900
950
1000
2.4
1.6
.8
0
0
10
20
30
40
50
60
70
80
90
100
Apparent age, Ma
Ar-39 released, cumulative percent

Figure 6.

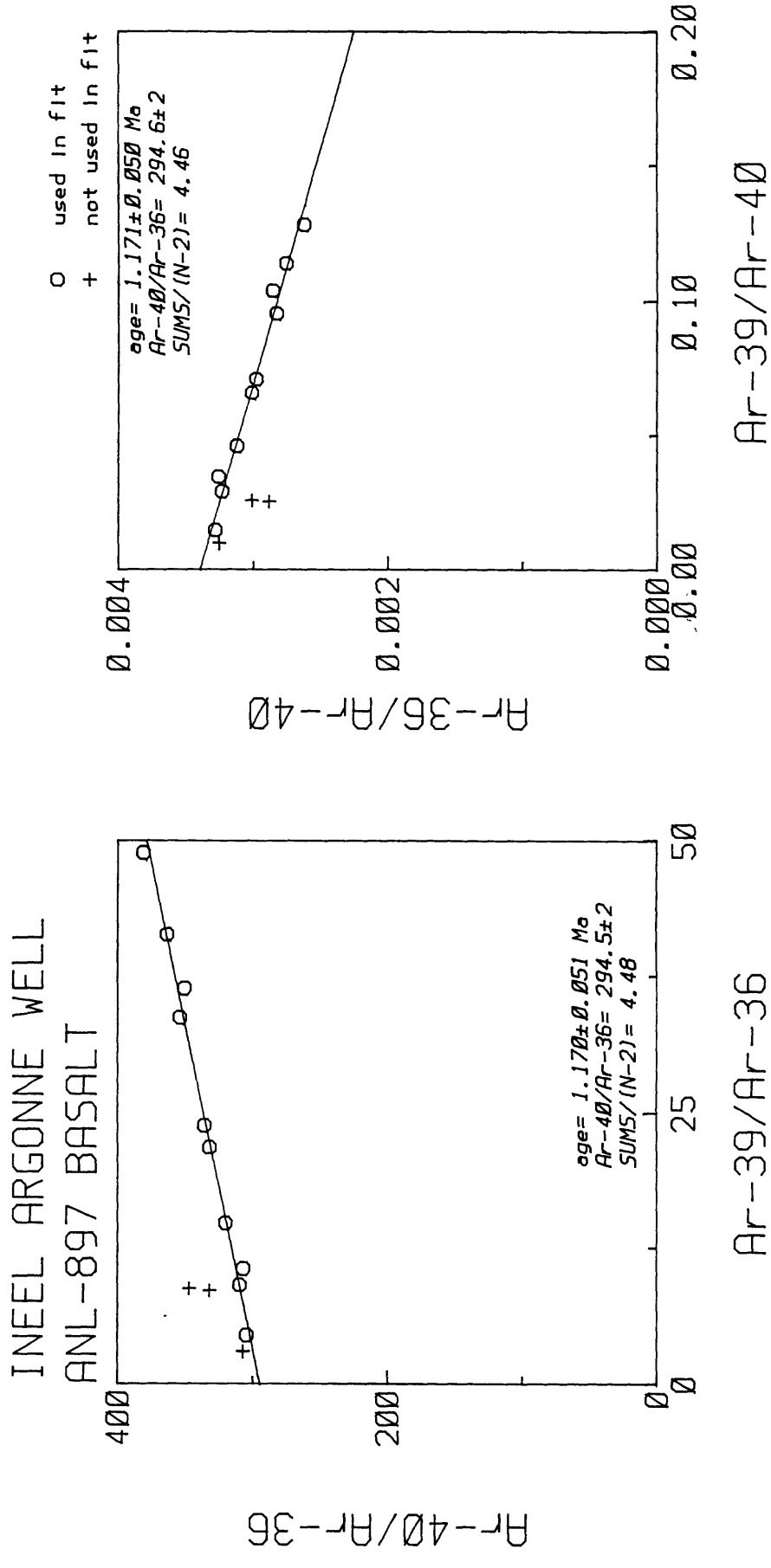
INEEL ARGONNE WELL
ANL-897 BASALT
Ar-40/Ar-36
400
200
0
0
25
50
Ar-39/Ar-36
age= 1.170±0.051 Ma
Ar-40/Ar-36= 294.5±2
SUMS/(N-2)= 4.48
Ar-36/Ar-40
0.004
0.002
0.000
0.00
0.10
0.20
Ar-39/Ar-40
o used in fit
+ not used in fit
age= 1.171±0.050 Ma
Ar-40/Ar-36= 294.6±2
SUMS/(N-2)= 4.46

Figure 7.

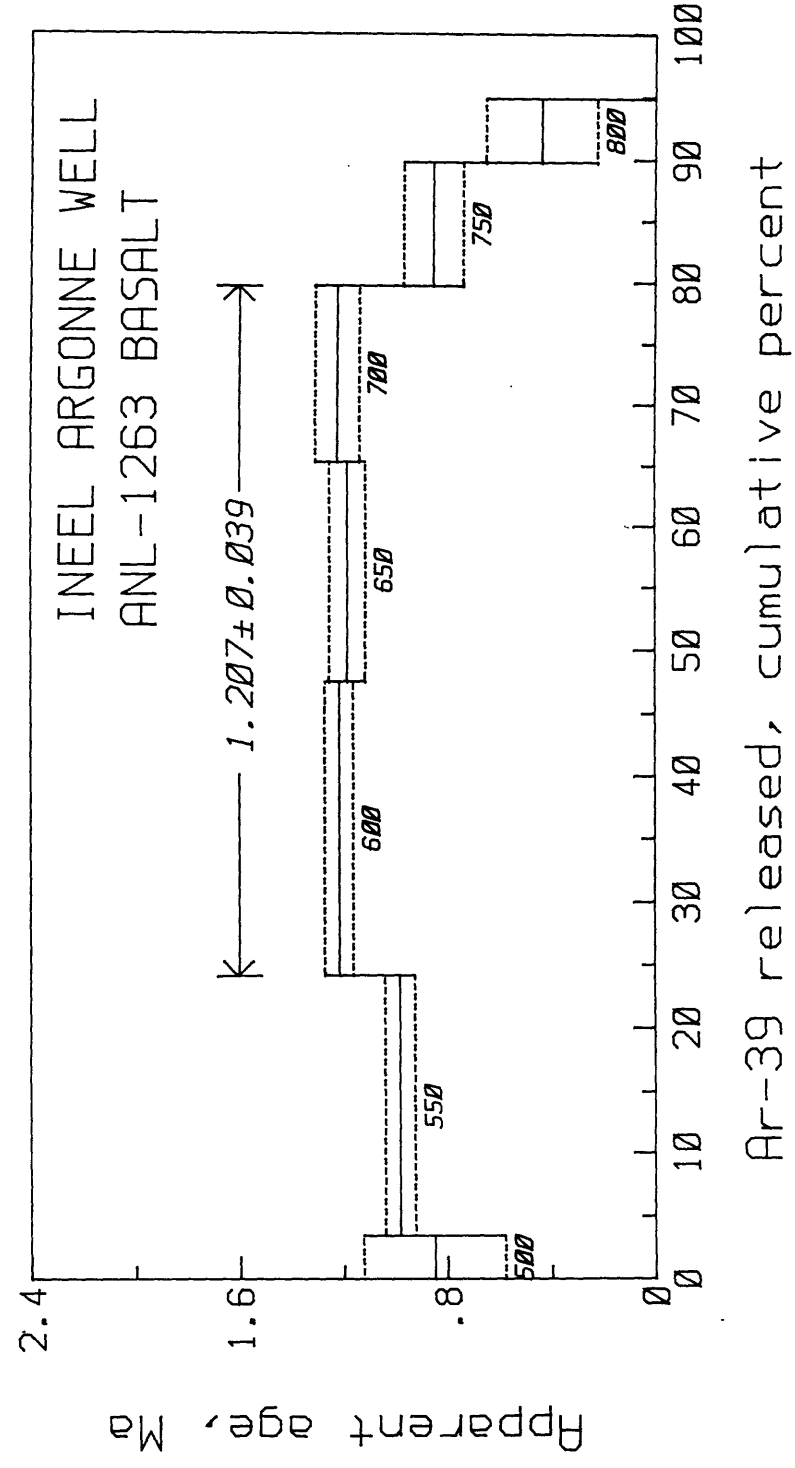
INEEL ARGONNE WELL
ANL-1263 BASALT
1.207±0.039
500
550
600
650
700
750
800
2.4
1.6
.8
0
0
10
20
30
40
50
60
70
80
90
100
Apparent age, Ma
Ar-39 released, cumulative percent

Figure 8.

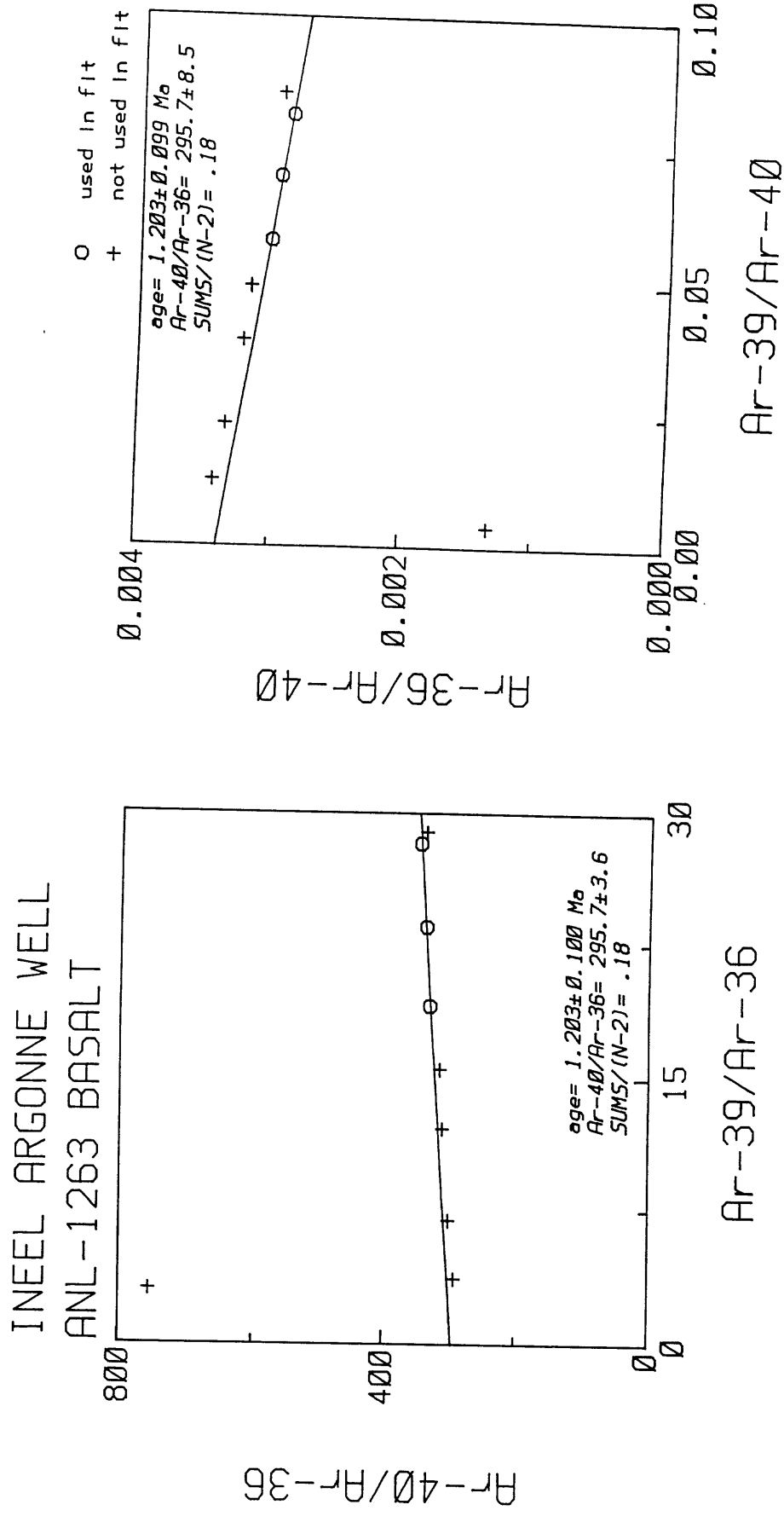
INEEL ARGONNE WELL
ANL-1263 BASALT
Ar-40/Ar-36
800
400
0
0
15
30
Ar-39/Ar-36
age= 1.203±0.100 Ma
Ar-40/Ar-36= 295.7±3.6
SUMS/(N-2)= .18
Ar-36/Ar-40
0.004
0.002
0.000
0.00
0.05
0.10
Ar-39/Ar-40
o used in fit
+ not used in fit
age= 1.203±0.099 Ma
Ar-40/Ar-36= 295.7±8.5
SUMS/(N-2)= .18

Figure 9.

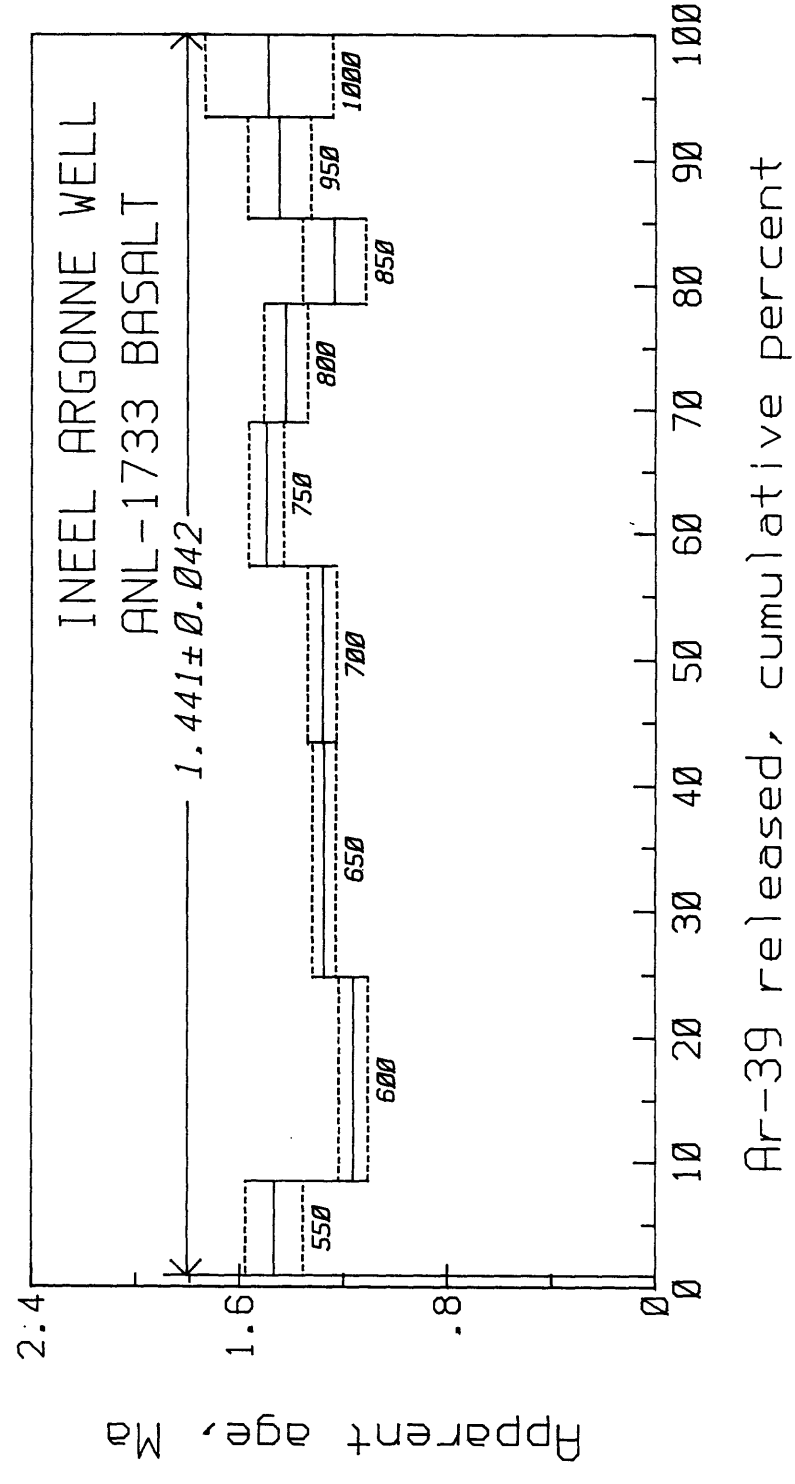
INEEL ARGONNE WELL
ANL-1733 BASALT
1.441±0.042
550
600
650
700
750
800
850
950
1000
2.4
1.6
.8
0
0
10
20
30
40
50
60
70
80
90
100
Apparent age, Ma
Ar-39 released, cumulative percent

Figure 10.

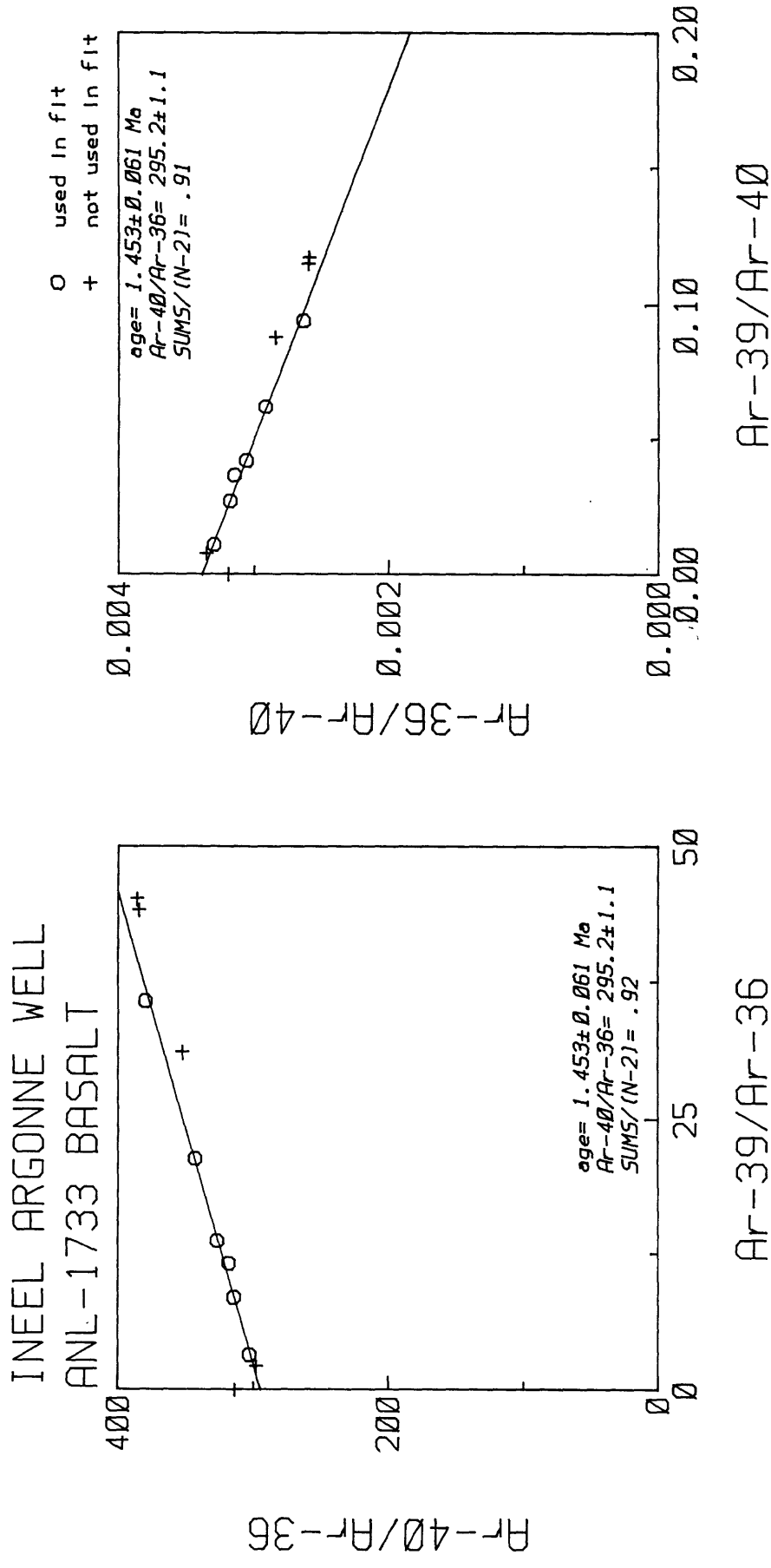
INEEL ARGONNE WELL
ANL-1733 BASALT
Ar-40/Ar-36
Ar-39/Ar-36
400
200
0
0
25
50
age= 1.453±0.061 Ma
Ar-40/Ar-36= 295.2±1.1
SUMS/(N-2)= .92
Ar-36/Ar-40
Ar-39/Ar-40
0.004
0.002
0.000
0.00
0.10
0.20
o used in fit
+ not used in fit
age= 1.453±0.061 Ma
Ar-40/Ar-36= 295.2±1.1
SUMS/(N-2)= .91

Figure 11.

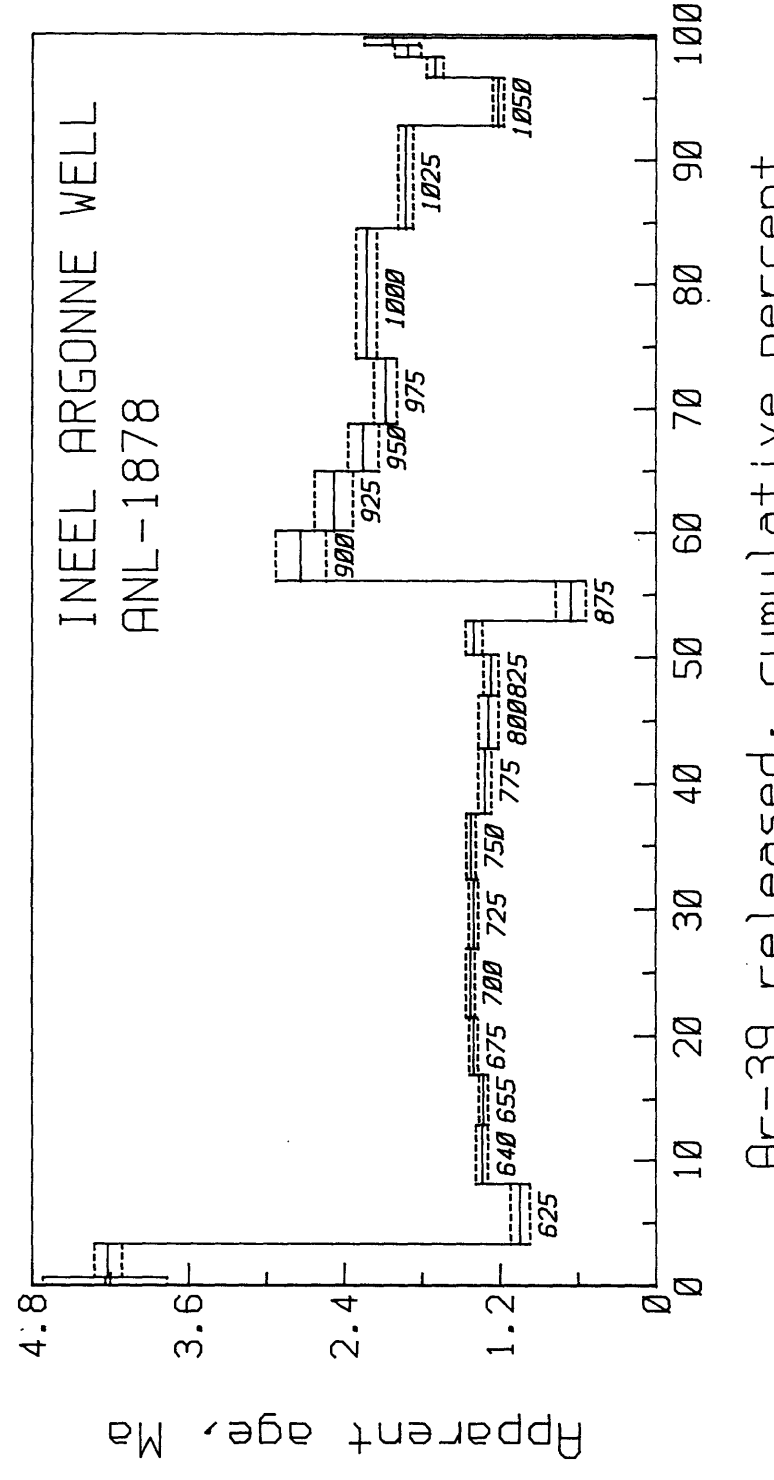
INEEL ARGONNE WELL
ANL-1878
Apparent age, Ma
Ar-39 released, cumulative percent
4.8
3.6
2.4
1.2
0
0
10
20
30
40
50
60
70
80
90
100
625
640
655
675
700
725
750
775
800
825
875
900
925
950
975
1000
1025
1050

Figure 12.

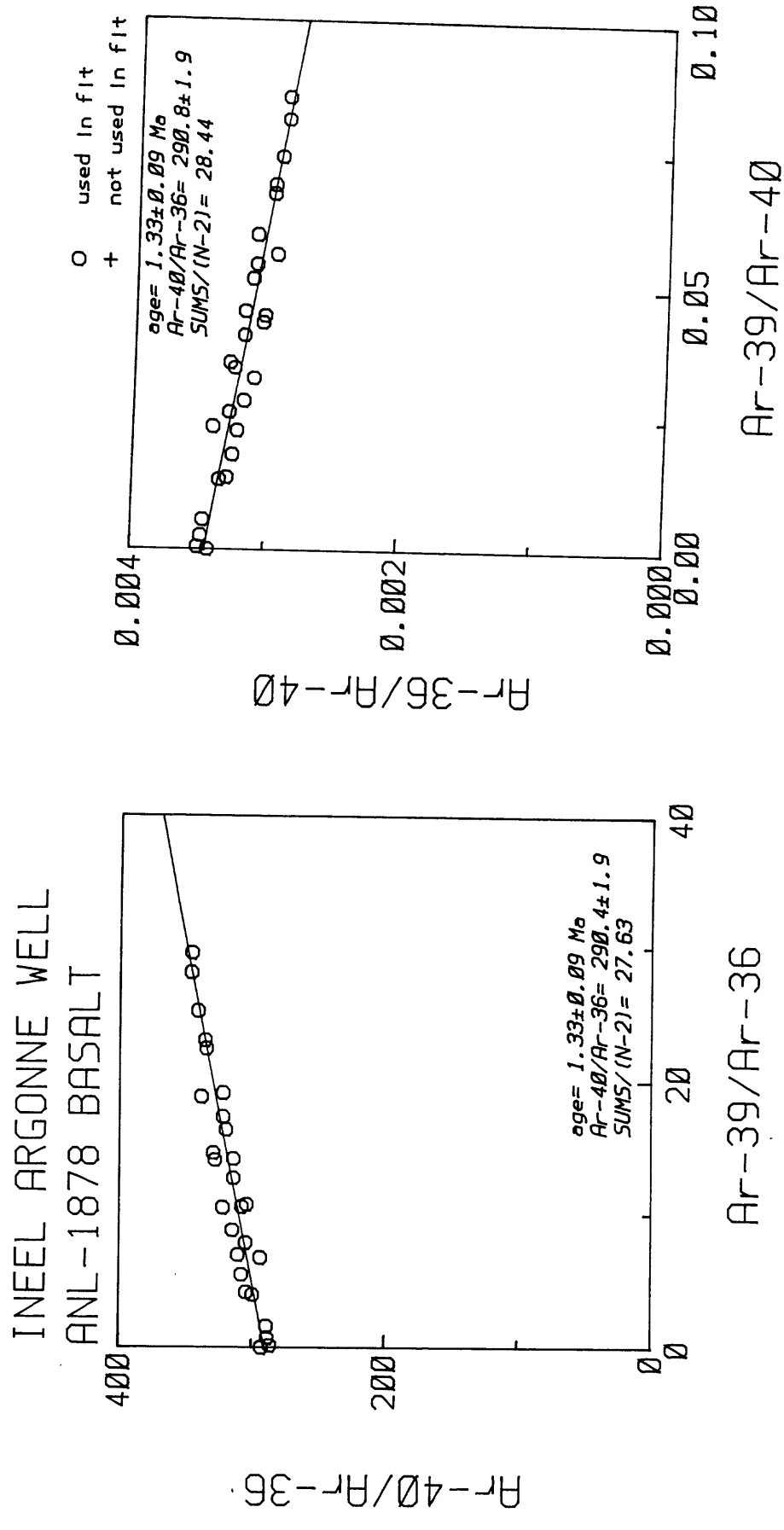
INEEL ARGONNE WELL
ANL-1878 BASALT
Ar-40/Ar-36
Ar-39/Ar-36
400
200
0
0
20
40
age= 1.33±0.09 Ma
Ar-40/Ar-36= 290.4±1.9
SUMS/(N-2)= 27.63
Ar-36/Ar-40
Ar-39/Ar-40
0.004
0.002
0.000
0.00
0.05
0.10
o used in fit
+ not used in fit
age= 1.33±0.09 Ma
Ar-40/Ar-36= 290.8±1.9
SUMS/(N-2)= 28.44

Figure 13.

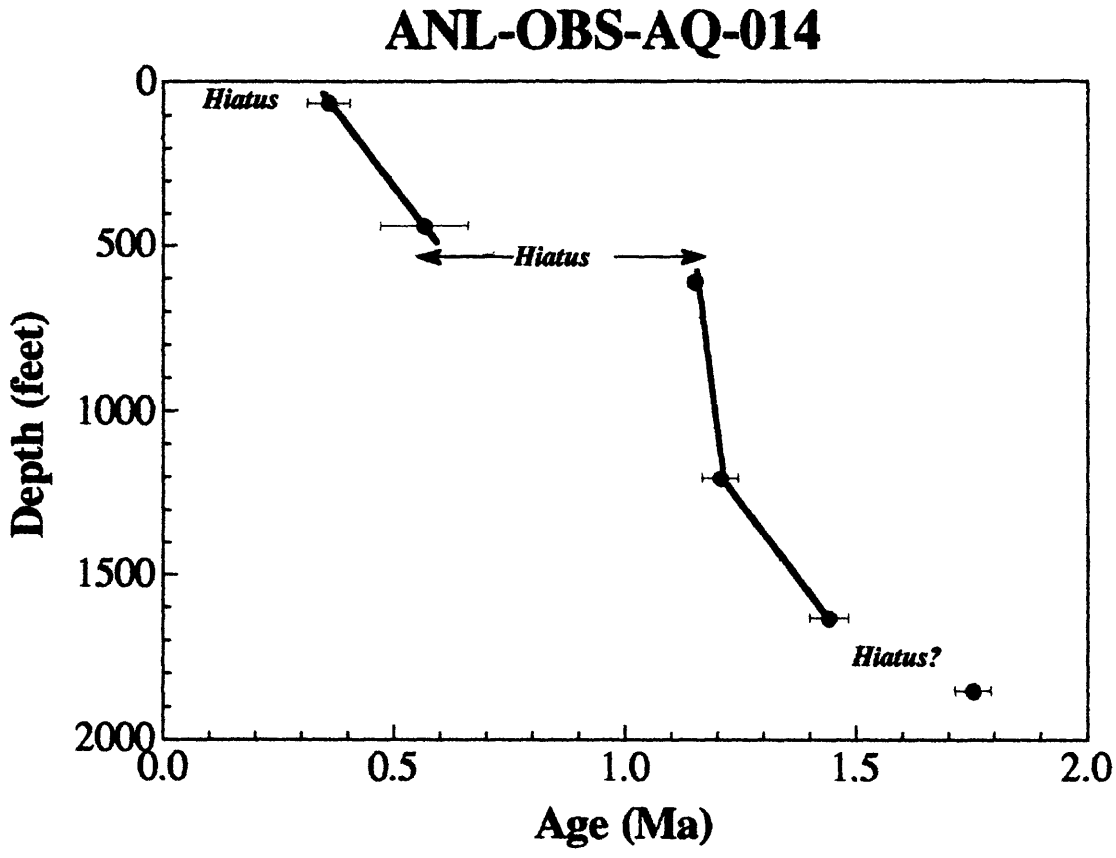
ANL-OBS-AQ-014
Hiatus
Hiatus
Hiatus?
Depth (feet)
0
500
1000
1500
2000
0.0
0.5
1.0
1.5
2.0
Age (Ma)